Catena 179 (2019) 129–138

Contents lists available at ScienceDirect

Catena

journal homepage: www.elsevier.com/locate/catena

Impacts on watershed-scale runoff and sediment yield resulting from synergetic changes in climate and vegetation

Shanghong Zhang[a,*], Zehao Li[a], Xiaoning Hou[a], Yujun Yi[b,*]

[a] Renewable Energy School, North China Electric Power University, Beijing 102206, China
[b] School of Environment, Beijing Normal University, Beijing 100875, China

ARTICLE INFO

Keywords:
Climate change
Vegetation cover change
Synergetic changes
Runoff
Sediment yield

ABSTRACT

This study investigates the relations between climate change and both runoff and sediment yield in watersheds and provides a scientific basis for water resources planning and design as well as watershed-scale soil and water conservation. The impact of climate change on runoff and sediment yield in a watershed does not occur in isolation, but is a synergistic process in which climate and vegetation jointly influence runoff and sediment yield. Previous studies have seldom addressed this synergistic effect. For this study, a regression model between climate factors (temperature and precipitation) and the Normalized Difference Vegetation Index (NDVI) was established using data from the Zhenjiangguan Watershed in China. By combining data on climate-driven changes in vegetation cover, the Soil and Water Assessment Tool (SWAT) model was built to simulate runoff and sediment yield in the watershed under two scenarios: changes in climate, and synergistic changes in climate and vegetation cover. The simulation results show that precipitation is the most sensitive factor affecting runoff and sediment yield; 10% change in annual precipitation can cause 10%–14% change in annual runoff and 17%–24% change in annual sediment yield. Temperature is also an important factor affecting runoff and sediment yield in the watershed. Each temperature increase of 0.7 °C can result in a decrease of 1.4%–2% in annual runoff and 2%–3.7% in annual sediment yield. This research reveals that accounting for synergetic change in vegetation has an impact on runoff and sediment yield results, and that the magnitude and nature of this influence vary among different combinations of temperature and precipitation changes. When temperature was kept constant, the effect of vegetation cover change caused by precipitation change on runoff and sediment yield was relatively small (only 0.9%–1.5% of the total change), and vegetation cover change inhibited the effects of precipitation change on runoff and sediment yield. When precipitation was kept constant, the effects of vegetation cover change caused by temperature change on runoff and sediment yield were relatively large (20%–30% of the total change), and vegetation cover change enhanced the effects of temperature change on runoff and sediment yield. This investigation considers the synergistic effects of climate and vegetation cover change, and thus further clarifies the extent to which climate change impacts water and ecological resources.

1. Introduction

Climate change has become a concern among the scientific community, governments, and the public. Climate change will inevitably affect the hydrological cycle and the temporal and spatial distribution of water resources (Zhou et al., 2011). These changes, in turn, may lead to soil erosion within watersheds along with other ecological and environmental problems (Shrestha and Wang, 2018; Wen et al., 2018; Andersen et al., 2014). Thus, assessing changes in runoff and sediment yield in the context of climate change and demonstrating the relations between climate change and both hydrological resources and ecological change can provide a scientific basis for designing, using, and managing water resource systems and help further watershed-scale soil and water conservation efforts (Pourmokhtarian et al., 2017).

The impacts of climate change on runoff and soil erosion also interact with the underlying surface factors that cause changes in runoff and sediment yield (Simonneaux et al., 2015; Serpa et al., 2015). Changes in the underlying surface include land-use changes caused by human activity; examples include land reclamation or conversion of farmland back to forests. These changes occur on a short timescale but can cause substantial changes in the underlying surface (Yu et al., 2011). However, changes in the underlying surface also include natural changes in land cover resulting from climate change, such as changes in vegetation cover due to changes in temperature and precipitation. This

* Corresponding authors.
E-mail addresses: zhangshanghong@ncepu.edu.cn (S. Zhang), yiyujun@bnu.edu.cn (Y. Yi).

https://doi.org/10.1016/j.catena.2019.04.007
Received 10 October 2018; Received in revised form 21 February 2019; Accepted 5 April 2019
Available online 13 April 2019
0341-8162/ © 2019 Elsevier B.V. All rights reserved.

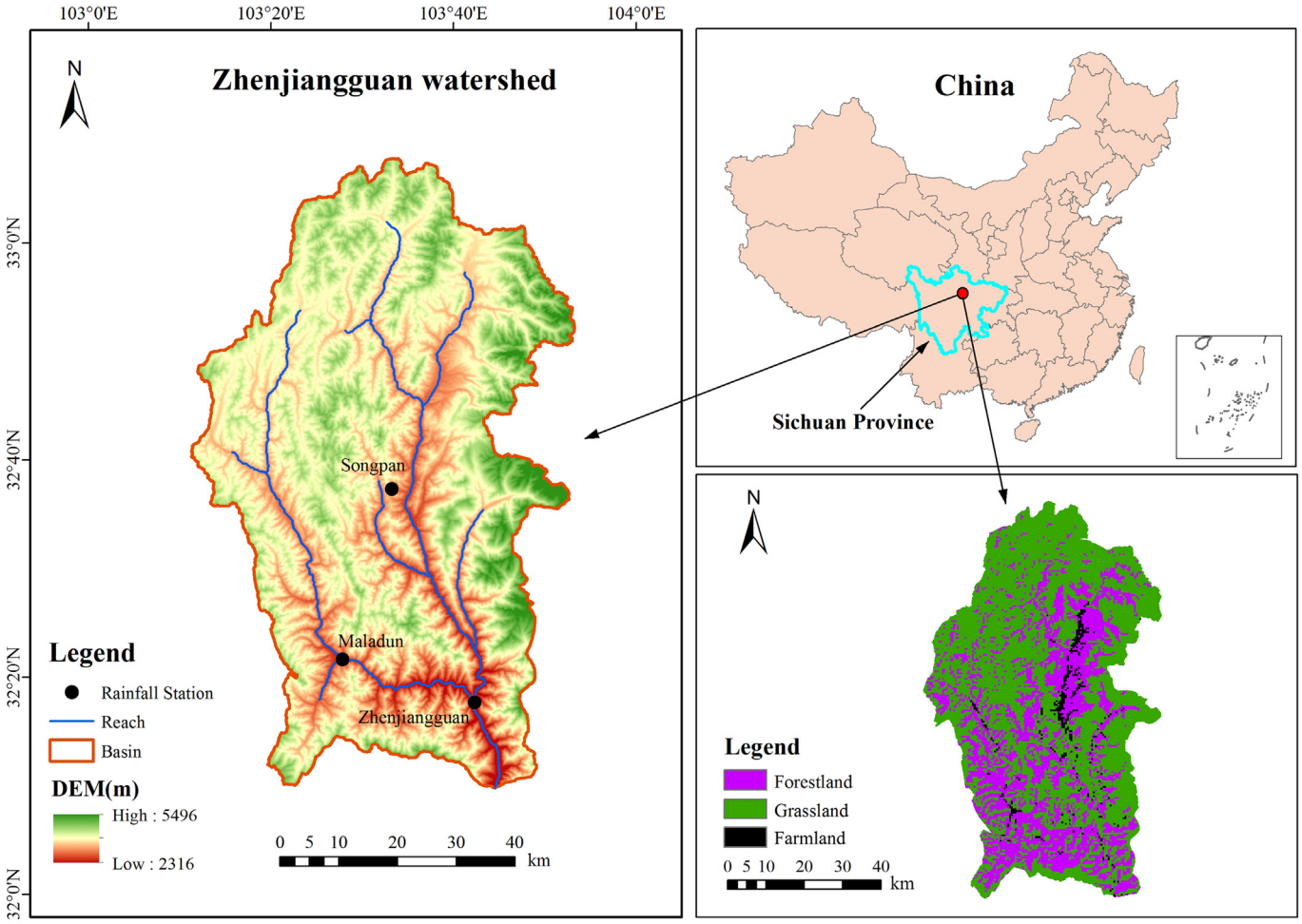

Fig. 1. Digital Elevation Model (DEM), rainfall stations, location, and land use/land cover in 2000 for the Zhenjiangguan Watershed.

type of change in the underlying surface occurs relatively slowly and is closely associated with climate change (Yan et al., 2013; Li et al., 2017). To study the impact of climate change on runoff and sediment yield in watersheds, it is necessary to analyze changes in vegetation cover factors as well as to identify the contribution rates of climatic changes and climate-driven vegetation cover changes to runoff and sediment yield.

Research regarding the impacts of climate change on runoff and sediment yield typically conforms to the following pattern: future climate scenario design, hydrological simulation, impact assessment. A distributed hydrological model can take into account the distribution characteristics of climatic conditions and surface vegetation cover, and therefore is a useful tool for quantifying the environmental impacts of climate and vegetation changes on runoff and sediment yield. Previous studies have assessed the direct impacts of climate change on runoff and sediment yield (Chen and Dudhia, 2001; Arpe et al., 2005; Li et al., 2013; Routschek et al., 2014; Zhang and Nearing, 2005). For example, Li et al. (2013) used the SIMHYD and GR4J hydrological models to analyze the impact of climate change on runoff for the Brahmaputra River. Their results showed that climate change would lead to a continuous increase in annual runoff. Routschek et al. (2014) investigated changes in soil erosion rates based on the A1B IPCC-scenario in Saxony, Germany and suggested that climate change would lead to a substantial increase in soil loss by 2050 and a partial decrease by 2100. Zhang and Nearing (2005) reported that changes in mean annual precipitation and mean annual temperature in central Oklahoma would cause considerable changes in runoff and soil erosion. Although these studies investigated the impact of climate change on runoff and soil erosion, most have used a constant underlying surface or only considered changes in land-use types. This approach lacks consideration for synergetic changes in vegetation cover caused by climate change.

Studies on the impacts of vegetation cover changes on runoff and sediment yield have mainly focused on two aspects: the trend of vegetation change and its driving mechanism. The impact of vegetation on runoff and sediment yield is evident during precipitation events. The plant canopy intercepts and redistributes rainfall, while the root system changes the soil configuration and enhances soil infiltration capacity (Kim et al., 2014). Regarding changes in vegetation cover, many researchers have used the Normalized Difference Vegetation Index (NDVI) or Leaf Area Index (LAI) to characterize vegetation coverage (Zoungrana et al., 2018; Senay and Elliott, 2000) and to study the relations between vegetation cover, runoff, and sediment in long time series (Du and Shi, 2013; Jin et al., 2008; Yu et al., 2006). For example, Zoungrana et al. (2018) applied NDVI data from Moderate-resolution Imaging Spectroradiometer (MODIS) images to monitor the dynamics of vegetation in the Burkina Faso savannah, western Africa and to assess the degradation of natural vegetation cover. Du and Shi (2013) analyzed the effects of precipitation and vegetation coverage on runoff and sediment yield in the Jinsha River Basin and concluded that runoff and sediment yield were positively correlated with precipitation and negatively correlated with NDVI. Zhou et al. (2013) incorporated remote-sensing-derived vegetation LAI into the rainfall–runoff model, which considerably improved the accuracy of hydrological process simulation in a forest catchment.

Although a number of studies have addressed the impacts of climate change or vegetation cover change on runoff and sediment yield, previous studies have not thoroughly considered the effects of climate

change on plant growth. Prior studies have based simulations on a constant underlying surface, but have neglected to take into consideration the synergistic effects between climate, vegetation, runoff, and sediment. Although the influence of climate change on vegetation is small in the short term, neglecting vegetation changes may reduce the reliability of simulation results when studying the responses of runoff and sediment yield to long-term climate change. Therefore, studying the different responses of runoff and sediment yield between these two different modes is conducive to more clearly and accurately predicting the trends of runoff and sediment yield in watersheds, which can provide a scientific basis for rational utilization of runoff resources and reduction of soil erosion under future climate change scenarios.

This paper establishes a regression model between climatic factors and vegetation cover factors and a distributed hydrological model (the Soil and Water Assessment Tool (SWAT)) with a physical basis, aimed at the following research objectives: (1) study the potential impacts of climate change on runoff and sediment yield in watersheds; (2) investigate the laws of vegetation cover change driven by climate change, and study the potential impacts of synergetic changes in climate and vegetation cover on runoff and sediment yield in watersheds; and (3) quantify the contributions of climate change factors and vegetation cover change factors to runoff and sediment yield variations.

2. Material and methods

2.1. Study area

The Zhenjiangguan Watershed (Fig. 1) is located in the northeast region of the Tibetan Plateau and is part of the Western Sichuan Plateau of China. The Zhenjiangguan Watershed covers 4500 km^2 and lies within 103°11′–103°54′E and 32°9′–33°9′N. The climate in the Zhenjiangguan Watershed is dry, with an average annual precipitation of 570 mm, and 80% of the annual precipitation occurs from May to October (Zhang et al., 2013b). Land cover in the Zhenjiangguan Watershed mainly includes grassland (65% of the total area) and forestland (32%). Areas of farmland, urban land, bare land, and water in the study area were too small to be included in this research. Climate change in this region has influenced water conditions as well as sediment production and transport in recent decades. Climate change has both a direct effect on runoff within river basins and a direct effect on soil erosion via changes in vegetation cover. According to remote sensing data from 1985 and 1997, the areas affected by soil erosion in Songpan county, located within the study area, increased at a rate of 19%, from 2713 to 3233 km^2 (Yao et al., 2006). The rate of soil erosion within the watershed has increased from slight to moderate to severe, and the problems of soil and water loss may continue to increase (Yao et al., 2006). Analyzing the response of runoff and sediment yield to synergetic changes in climate and vegetation cover can provide a reference for assessing ecological improvements along with soil and water conservation efforts in the Zhenjiangguan Watershed. In addition, this study did not include Land Use/Land Cover (LULC) changes because the conversions of LULC classes in the study area were not considerable based on the examination of LULC maps in the past three periods (1986, 1995, and 2000).

2.2. Data sources

Sources of the spatial and attribute data and details about the spatial and temporal resolution of the analysis are provided in Table 1. The NDVI data used in this study are third-generation normalized difference vegetation index data from the National Aeronautics and Space Administration (NASA) generated by the Advanced Very High Resolution Radiometer (AVHRR) sensor. The 15-d NDVI data were subjected to radiometric calibration and geometric correction to remove effects not associated with variations in vegetation and were preprocessed using the Maximum Value Composite (MVC) to generate monthly values of

Table 1
Time, resolution, and source information data for this study.

Data type	Name	Time	Spatial/temporal resolution	Source
Spatial data (measured)	DEM	2009	30 m	Computer Network Information Center, Chinese Academy of Sciences (http://www.gscloud.cn)
	AVHRR NDVI	1982–2003	1/12°	National Earth System Science Data Sharing Infrastructure (http://www.geodata.cn)
	Soil data	2009	1:1000000	Environment and Ecological Science Data Center for West China (http://westdc.westgis.ac.cn)
	Land use map of Sichuan Province	2000	1:100000	National Earth System Science Data Sharing Infrastructure (http://www.geodata.cn)
Hydrological data (measured)	Runoff, Sediment	1985–2005	Daily	Zhenjiangguan hydrologic station
Meteorological data	Precipitation, Max & Min temperature, Relative humidity, Wind speed	1978–2006	Daily	Rainfall data: Three rainfall stations; Meteorological data: http://data.cma.cn

the NDVI (Fontana et al., 2012; Beck et al., 2011).

2.3. NDVI-climate factor regression model

NDVI is a remote-sensing index that quantifies vegetation growth and vegetation coverage, with the NDVI value increasing as vegetation coverage increases (Pouchin et al., 2002). Although the correlation between NDVI and climate has been widely documented on a regional scale (Fu and Burgher, 2015), the degree of correlation varies between regions and vegetation types. The correlation between the NDVI and climate is primarily determined by calculating and testing the Pearson correlation coefficient (Zhang et al., 2013a). The Pearson correlation coefficient is computed as:

$$R_{xy} = \frac{\sum_{i=1}^{n}[(x_i - \overline{X})(y_i - \overline{Y})]}{\sqrt{\sum_{i=1}^{n}(x_i - \overline{X})^2}\sqrt{\sum_{i=1}^{n}(y_i - \overline{Y})^2}}, \quad (1)$$

where x_i and y_i are the values of data series x and y, respectively; n is the number of data values; $\overline{X}$ and $\overline{Y}$ are the average values of x and y; and R_{xy} is the correlation coefficient between x and y.

Many studies have shown that plants respond most sensitively to climate change during their vigorous growth period, whereas plants respond slowly to climate change in other periods (Tang et al., 2017; Pang et al., 2017). To more clearly analyze the interannual variations in climate and NDVI in the study area, and to show the response of vegetation growth to climate change, it is necessary to investigate the correlation between the maximum NDVI and climate factors (temperature and precipitation) in the growing season every year. In this study, the maximum NDVI of the growing season occurs between July and September. Therefore, mean temperature and precipitation from July to September during 1982–2003 at three rainfall stations (Fig. 1) within the study area were counted. The temperature and precipitation of the total study area are average values from these three rainfall stations. Mean NDVI from July to September during 1982–2003 were obtained using ArcGIS10.2 software, which was applied to perform projections and transformations, mask extraction, and raster calculation on the original NDVI data.

Because of the lag in vegetation response to climate change, a lag correlation coefficient was used to express the time-delay effect on the NDVI resulting from changing climate factors (Paus, 2013):

$$R^* = max\{R_0, R_1, R_2 \cdots R_{n-1}, R_n\}, \quad (2)$$

where R^* is the lag correlation coefficient, and R_n represents the correlation coefficients between the NDVI and climate variables in n month (s) prior. Partial correlation analysis was used to calculate the lag correlation coefficient between the NDVI and climatic variables (mean temperature and precipitation), and the calculations resulted in $R^* = R_1$. The results indicate that the lag period of vegetation NDVI response to climatic factors was 1 month, and that the correlation coefficients reached their maximum at this time (the maximum correlation coefficients R_1 between NDVI and mean temperature and precipitation were 0.64 and 0.66, respectively).

The NDVI-climate factor regression model was built using IBM SPSS Statistics 20 software. Mean NDVI from July to September during 1982–2003 were used as the dependent variable, corresponding mean temperature and precipitation were used as independent variables, and the model was built using linear regression. Based on the analysis results, the quality of the established binary linear regression model was evaluated to ensure the applicability of this model.

2.4. Hydrological model

2.4.1. SWAT model

The SWAT model is an agro-hydrological, watershed-scale model developed by United States Department of Agriculture-Agricultural Research Service (USDA-ARS) (Neitsch et al., 2011). The SWAT model has a strong physical foundation and can make continuous calculations at daily intervals. It takes into account the impacts of climate change, underlying surface conditions, and various water resource management measures to simulate hydro-physical processes, including water, sediment, and agricultural chemical yields in complex watersheds (Dechmi et al., 2012; Cho et al., 2012). The SWAT extension for ArcGIS software, called ArcSWAT, was used in this research to calculate runoff and sediment yield in the Zhenjiangguan Watershed.

For the SWAT model, the entire watershed was divided into several sub-basins and then further divided into multiple hydrological response units (HRUs) based on land use, soil, and slope. One HRU refers to the smallest hydrological unit with similar land and hydrological characteristics. HRUs are used as the basic calculation unit in the SWAT model (Flügel, 1995).

The plant growth component of SWAT is a simplified version of the EPIC plant growth model (Neitsch et al., 2011). It uses the same growth equations for all the plants, and the difference in growth between different plant species is determined by specific parameters (such as the LAI) in the plant growth database. The leaf area development of plants can cause changes in runoff and soil erosion in watersheds by affecting physical processes such as evapotranspiration, rainfall interception, and infiltration. In this research, vegetation information obtained from remote sensing data was integrated into the plant growth database of SWAT.

2.4.2. Model calibration and validation

The model was calibrated and validated with 21 years of monthly observed discharge and sediment yield from the Zhenjiangguan hydrological station at the whole watershed outlet. The simulation period of the model was from 1980 to 2005, of which 1980–1984 was set as the model warm-up period, 1985–1995 was set as the model calibration period, and 1996–2005 was set as the model validation period.

The percentage bias (PBIAS), coefficient of determination (R^2), and Nash and Sutcliffe (1970) efficiency coefficient (NSE) are often used to evaluate the quality of hydrological models. These parameters are computed as follows:

$$PBIAS = \frac{\sum_{i=1}^{n}(Q_{oi} - Q_{si})}{\sum_{i=1}^{n}(Q_{oi})} \times 100\%, \quad (3)$$

$$NSE = 1 - \frac{\sum_{i=1}^{n}(Q_{oi} - Q_{si})^2}{\sum_{i=1}^{n}(Q_{oi} - Q_{avg})^2}, \quad (4)$$

$$R^2 = \frac{[\sum_{i=1}^{n}(Q_{oi} - Q_{avg})(Q_{si} - Q'_{avg})]^2}{\sum_{i=1}^{n}(Q_{oi} - Q_{avg})^2 \sum_{i=1}^{n}(Q_{si} - Q'_{avg})^2}, \quad (5)$$

where n is the number of the data values; Q_{oi} and Q_{si} are the observed and simulated values at month i, respectively; and Q_{avg} and Q_{avg}' are the mean values of the observed data and simulated values, respectively.

The PBIAS was used to evaluate the overall deviation between the simulated and observed values. The R^2 and NSE were used to evaluate the quality of the model and measure the goodness of fit between the simulated and observed values. The closer these two coefficients are to 1, the closer the simulated values are to the observed values (Yesuf et al., 2015). Thus, the accuracy of the simulation is satisfactory if the discharge calibration meets $|PBIAS| < 20\%$, $R^2 > 0.6$, and $NSE > 0.5$, and if the sediment calibration meets $|PBIAS| < 30\%$, $R^2 > 0.6$, and $NSE > 0.5$ (Moriasi et al., 2007).

2.5. Modeling under different scenarios

In this study, two different scenarios (changes in climate, and synergistic changes in climate and vegetation cover) were established to investigate the response of runoff and sediment yield in different scenarios and to quantify the contributions of various factors to runoff and sediment yield in the watershed.

2.5.1. Changes in climate

The establishment of climate change scenarios in this paper is based on a hypothesis method. Hu et al. (2012) simulated climate change for the mid-21st century in China using the IPCC A1B scenario, and the results showed that the surface temperature in southwest China would increase at a rate of approximately 0.7 °C/10 yr, and that precipitation would increase or decrease at a rate of 10%/10 yr. To make the temperature and precipitation changes within a reasonable range, this study referred to the research results of Hu, and set the future climate change scenario in the study area as follows: the change in precipitation is −20%, −10%, 0%, +10%, and + 20% of precipitation for the base year 2000; and the temperature increases by 0 °C, 0.7 °C, 1.4 °C, and 2.1 °C from the temperature in 2000.

The different climate change scenarios in the SWAT model can be completed by modifying the temperature and precipitation data in the meteorological database. Based on actual temperature and precipitation data for 2000, 20 groups of temperature and precipitation data were added to the meteorological database according to the established climate change scenarios. Without considering changes in vegetation cover, the simulations for these scenarios were based on the vegetation conditions of the Zhenjiangguan Watershed in 2000.

2.5.2. Synergistic changes in climate and vegetation cover

In this scenario, changes in climatic factors (temperature and precipitation) will lead to changes in vegetation cover, which will impact water and sediment processes. Based on the climate and vegetation conditions in the Zhenjiangguan Watershed in 2000, the predicted NDVI values corresponding to climate change scenarios were calculated using the NDVI-climate factors regression model. Then, the predicted NDVI values were converted into LAI based on an empirical relationship (see Eq. (6)) derived by Li et al. (2005). Finally, the obtained LAI values were added into the plant growth database of SWAT to investigate the response of runoff and sediment yield in this scenario.

$$Y = 12.274X - 3.917, \quad (6)$$

where Y are LAI values and X are NDVI values.

3. Results and discussion

3.1. Regression analysis of NDVI-climate factors

The analysis results of the IBM SPSS Statistics 20 software on the NDVI-climate factors regression model were summarized in this section. The multiple correlation coefficient $R = 0.75$ indicates that the vegetation NDVI is closely related to climatic factors. The adjusted coefficient of determination $R^2 = 0.51$ indicates that the climatic factors in the regression equation explain 51% of the variation in the vegetation NDVI value. The standard error of the estimate, which indicates the relative deviation between observed and estimated values, was relatively low (0.035). Regarding the analysis of variance, the probability of F significant statistics, Sig.F < 0.05, indicates that there was a significant linear relation between the dependent variable (NDVI) and the independent variables (mean temperature and precipitation) at the $P < 0.05$ significance level.

In Table 2, the partial regression coefficients corresponding to temperature and precipitation represent the degree to which independent variables influenced each dependent variable separately. Sig.T represents the significance of the t-test for partial regression coefficients, and all are < 0.05, which indicates that all independent variables had a significant effect on the dependent variable. Collinearity statistics (tolerance and Variance Inflation Factor (VIF)) were used to determine whether there were collinearity issues between independent variables. When the tolerance is < 0.1, or when VIF is > 10, there may be collinearity issues between the independent variables. As listed in Table 2, the results indicate a tolerance equal to 0.72 (or VIF equal to 1.38), and thus demonstrate that collinearity is not significant.

Table 2
Partial regression coefficients and collinearity statistics.

Parameter	Partial regression coefficients	The probability of T significant statistics (Sig.T)	Collinearity statistics	
			Tolerance	VIF
T (temperature)	0.037	0.035	0.72	1.38
P (precipitation)	0.00085	0.023	0.72	1.38

Fig. 2 shows the regression standardized residuals and normal P-P plot of regression standardized residuals. These results demonstrate a normal distribution for the standardized residuals.

This analysis demonstrates that the NDVI-climate factor regression model had high accuracy and reliability. The linear regression equation for NDVI, temperature (T), and precipitation (P) was calculated as:

$$NDVI = 0.064 + 0.037 \times T + 0.00085 \times P. \quad (7)$$

This regression equation provides a basis for predicting NDVI values under different climate change scenarios.

3.2. LAI values for different land-use classes under different climate scenarios

The main land-use classes in the study area are grassland and forestland, accounting for 65% and 32% of the total area, respectively. The NDVI values corresponding to different land-use classes are different. This study used the Zonal Statistics tool of ARCGIS 10.2 to extract NDVI values for different land-use classes. Table 3 lists the average NDVI values for forestland and grassland from July to September in the 2000 land-use map based on the raster pixel scale.

As seen in Table 3, the NDVI values for forestland are larger than those for grassland. The standard deviations of raster cell values of NDVI relative to each LULC class are small. This result implies that the spatial distribution of NDVI values that correspond to the same LULC class is relatively stable and that the statistical results are highly representative. By using the established NDVI-climate factors regression model and the empirical conversion from NDVI to LAI (Li et al., 2005), the maximum LAI values of the growing season corresponding to each group of climate change scenarios were calculated, as shown in Table 4.

3.3. SWAT model calibration and validation

The Soil and Water Assessment Tool Calibration and Uncertainty Procedure (SWAT-CUP) was used for model calibration and validation. The Sequential Uncertainty Fitting Program (SUFI-2) in the SWAT-CUP package (Abbaspour et al., 2007) was selected for parameter optimization because of its high efficiency in watershed-scale application. The global sensitivity analysis showed that the sensitivity of seven runoff-related parameters and two sediment-related parameters were higher than the other parameters (see Table 5). These parameters were then adjusted to calibrate the model by using the auto-calibration extension of SWAT 2012. Table 5 lists the ranges and fitted values of these sensitive parameters.

The quality of the SWAT model was evaluated by comparing simulated monthly values of discharge and sediment yield with the observed monthly values. The results of the calibration and validation of the discharge and sediment simulations are shown in Figs. 3 and 4, respectively. Table 6 lists the results from the three evaluation indices for monthly discharge and sediment yield during the calibration and validation periods.

Figs. 3 and 4 demonstrate that the overall fitting degrees of the simulated and observed values for discharge and sediment yield are very high. Table 6 indicates that those evaluation index values are considered “satisfactory” according to general performance category by Moriasi et al. (2007). Thus, this model can be considered suitable for analyzing variability of runoff and sediment yield in the Zhenjiangguan

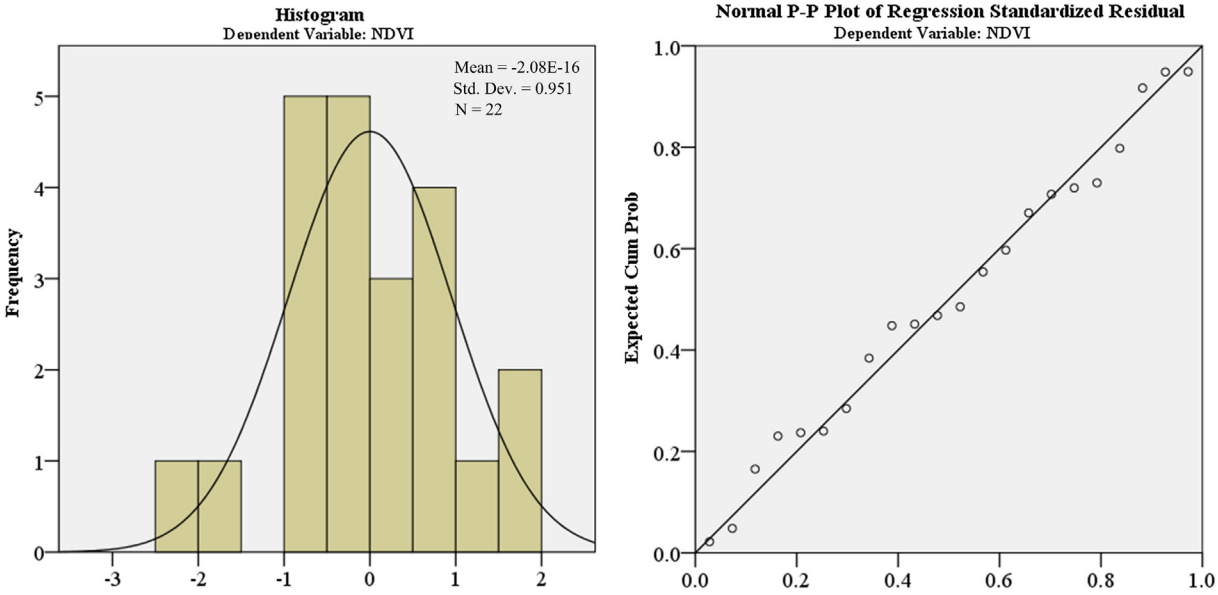

Fig. 2. The regression standardized residuals and normal P-P plot of regression standardized residuals.

Table 3
NDVI values of land use classes and statistical standard deviations in the 2000 land use map.

Land use classes	NDVI value	Standard deviation
Forestland	0.650	0.084
Grassland	0.558	0.130

Table 4
The maximum LAI values of the growing season for forestland and grassland under different climate change scenarios.

Land use classes	Precipitation	Temperature			
		T	T + 0.7	T + 1.4	T + 2.1
Forestland	P × (1 − 20%)	3.70	4.24	4.78	5.32
	P × (1 − 10%)	3.85	4.39	4.93	5.47
	P	4.01	4.54	5.08	5.62
	P × (1 + 10%)	4.15	4.69	5.23	5.77
	P × (1 + 20%)	4.30	4.84	5.38	5.92
Grassland	P × (1 − 20%)	2.77	3.18	3.58	3.99
	P × (1 − 10%)	2.89	3.29	3.70	4.10
	P	3.00	3.41	3.81	4.22
	P × (1 + 10%)	3.11	3.52	3.92	4.33
	P × (1 + 20%)	3.23	3.63	4.04	4.44

Watershed under different scenarios.

3.4. The responses of runoff and sediment yield under different scenarios

3.4.1. Changes in climate

Twenty groups of climate scenarios were simulated using the calibrated and validated SWAT model, and all of these scenarios adopted the vegetation conditions of the Zhenjiangguan Watershed in 2000. Table 7 lists the simulated values of total annual runoff and sediment yield at the outlet of the whole watershed.

From the analysis of the simulation results under the scenarios only considering change in climate (see Table 7), it was found that in the case of constant temperature, for every 10% increase in precipitation, annual runoff in the watershed increased by 190–213 million m^3 (accounting for about 10%–14% of the total annual runoff), and annual sediment yield increased by 75–117 thousand tons (accounting for about 17%–24% of the total annual sediment yield). In the case of constant precipitation, for every 0.7 °C increase in temperature, the annual runoff in the watershed decreased by 21–29 million m^3 (accounting for about 1.4%–2% of the total annual runoff), and the annual sediment yield decreased by 7–15 thousand tons (accounting for about 2%–3.7% of the total annual sediment yield). Thus, precipitation is the fundamental factor in the formation of runoff. Changes in precipitation can significantly change runoff, and there is a synchronous increasing or decreasing trend between these two parameters. Increase of

Table 5
Sensitivity analysis and calibration results of SWAT-CUP for runoff and sediment parameters.

	No	Name	Description	Range	Method	Fitted value
Runoff-related sensitive parameters	1	CN2	SCS runoff curve number for moisture condition II	± 25%	Relative	+15%
	2	SOL_AWC	Available water capacity of the soil layer (mm/mm soil)	± 30%	Relative	−7.7%
	3	GWQMN	Threshold depth of water in the shallow aquifer required for return flow to occur (mm)	0–5000	Absolute	−838
	4	GW_REVAP	Groundwater 'revap' coefficient	0.02–0.2	Absolute	+0.025
	5	REVAPMN	Threshold dept. of shallow aquifers evaporation/deep aquifer percolation (mm)	0–500	Absolute	−283
	6	RCHRG_DP	Deep aquifer percolation fraction	0–1	Absolute	+0.02
	7	ALPHA_BF	Baseflow alpha factor (days)	0–1	Absolute	+0.429
Sediment- related sensitive parameters	1	SPCON	Linear parameter for calculating the channel sediment routing	0.0001–0.01	Replace	0.001
	2	SPEXP	Exponent parameter for calculating the channel sediment routing	1–1.5	Replace	1.1

Note: Relative: multiplies the existing value with (1 + the given value). Absolute: adds the given value to the existing value. Replace: replaces the existing value with the given value.

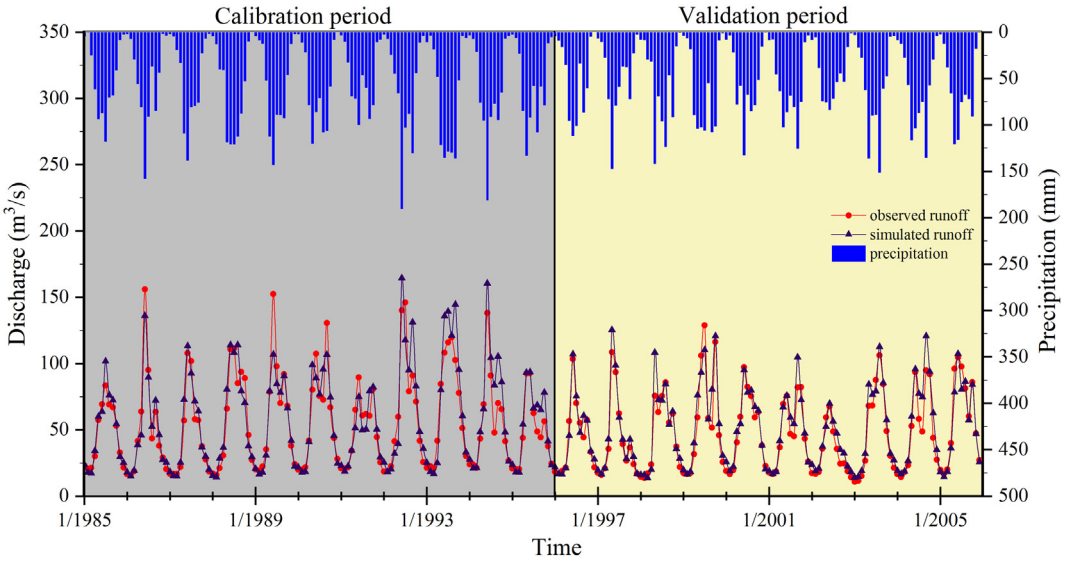

Fig. 3. Comparison of observed and simulated values for discharge during the calibration and validation periods.

precipitation leads to increase of runoff and surface scouring intensity, and ultimately also leads to the increase of sediment yield. Therefore, precipitation is the most sensitive factor affecting runoff and sediment yield in watersheds. Temperature is also an important factor affecting runoff and sediment yield in watersheds; increase in temperature will cause an increase in evapotranspiration as well as an increase in soil moisture deficit (Seneviratne et al., 2010; Vicente-Serrano et al., 2013), resulting in decreases in runoff and sediment yield.

3.4.2. Synergistic changes in climate and vegetation cover

With the other parameters of the SWAT model kept unchanged, only the leaf area development parameters corresponding to climate change were changed to simulate 20 groups of climate and vegetation synergistic change scenarios. The simulation results are shown in Table 7.

The differences of annual runoff and sediment yield under the two scenarios (changes in climate, and synergistic changes in climate and vegetation cover) were calculated, and the percentages of these differences to total change (the simulated value of each climate and vegetation synergistic change scenario minus the simulated value for 2000) were calculated. The results are listed in Fig. 5 and Table 8.

Table 6
Three evaluation indices of discharge and sediment yield for the calibration and validation periods.

Evaluation index	Discharge		Sediment yield	
	Calibration	Validation	Calibration	Validation
PBIAS	4.9%	6.9%	8.2%	10.3%
R^2	0.88	0.87	0.83	0.81
NSE	0.85	0.84	0.72	0.70

As shown in Table 7 and Fig. 5, there are differences in annual runoff and sediment yield between the climate change and climate and vegetation synergistic change scenarios, which indicates that vegetation changes driven by climate changes have an impact on runoff and sediment yield in the watershed. The magnitude of these differences varies with different combinations of temperature and precipitation. Runoff and sediment yield are negatively correlated with vegetation cover, and the increase of vegetation coverage can effectively reduce runoff and sediment yield in the watershed. When the temperature was

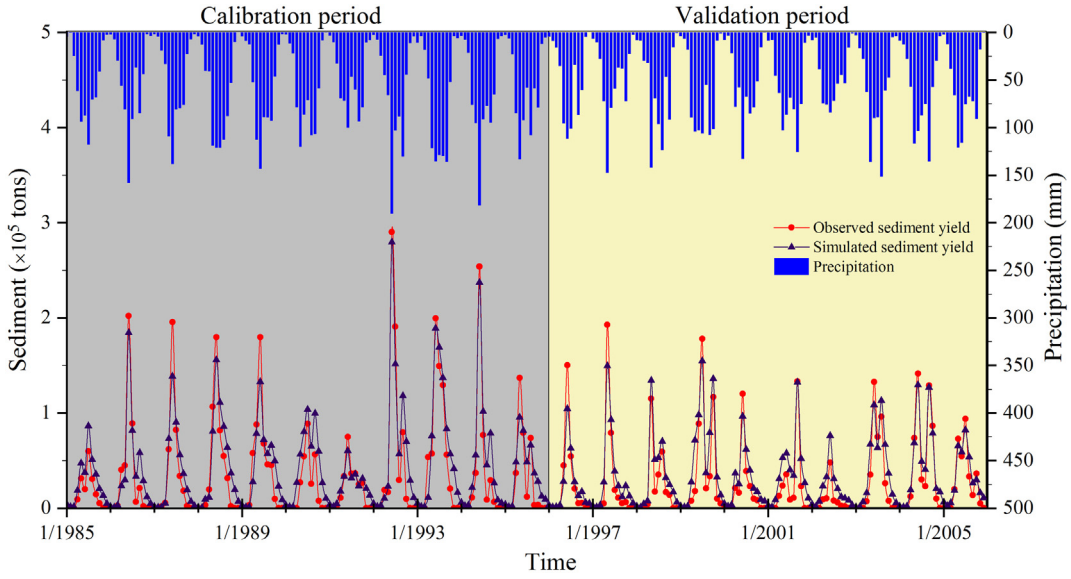

Fig. 4. Comparison of observed and simulated values for sediment yield during the calibration and validation periods.

Table 7
Simulated values of total annual runoff and sediment yield in the Zhenjiangguan Watershed, under two different scenarios (changes in climate, and synergistic changes in climate and vegetation cover).

	Precipitation	Temperature							
		T		T + 0.7		T + 1.4		T + 2.1	
		Climate changes	Synergistic changes	Climate changes	Synergistic changes	Climate changes	Synergistic changes	Climate changes	Synergistic changes
Annual runoff ($\times 10^6$ m^3)	P × (1 − 20%)	1197	1202	1173	1169	1154	1142	1133	1112
	P × (1 − 10%)	1393	1396	1367	1360	1347	1331	1323	1299
	P	1592	1592	1566	1555	1543	1524	1518	1490
	P × (1 + 10%)	1804	1801	1775	1762	1751	1729	1725	1693
	P × (1 + 20%)	2017	2012	1988	1972	1963	1938	1935	1900
Annual sediment yield (metric tons)	P × (1 − 20%)	259,302	260,816	250,123	248,813	243,036	238,981	235,851	228,391
	P × (1 − 10%)	338,919	340,175	328,122	325,501	320,245	314,069	310,642	301,882
	P	430,702	430,702	418,714	413,905	407,330	401,212	397,282	385,971
	P × (1 + 10%)	538,830	537,693	524,367	517,086	511,876	501,591	498,204	485,691
	P × (1 + 20%)	655,989	653,872	641,703	634,279	628,736	615,782	613,256	595,721

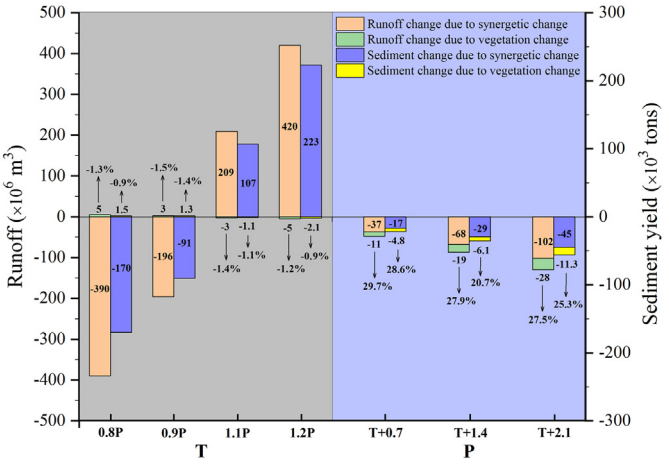

Fig. 5. Annual runoff and sediment yield changes caused by vegetation changes and their percentages to total changes while temperature or precipitation are kept constant.

kept constant, the differences of annual runoff and sediment yield caused by vegetation changes due to 10% change in annual precipitation were 0.9%–1.5% of the total changes, and all were negative. Thus, the effects of vegetation cover changes caused by precipitation changes on runoff and sediment yield were relatively small. The negative percentages indicate that vegetation cover changes inhibited the effects of precipitation changes on runoff and sediment yield. When the precipitation was kept constant, the differences of annual runoff and sediment yield caused by vegetation changes due to 0.7 °C change in temperature were 20%–30% of the total changes, and all were positive. These results imply that the effects of vegetation cover changes caused by temperature changes on runoff and sediment yield were relatively large. The positive percentages indicate that vegetation cover changes enhanced the effects of temperature changes on runoff and sediment yield. For example, increase in evapotranspiration caused by increase in temperature reduced runoff and sediment yield in watersheds, whereas increase in vegetation cover caused by increase in temperature also reduced runoff and sediment yield. Therefore, vegetation cover changes enhanced the effects of temperature changes on runoff and sediment yield. Similarly, the same enhancement effect also occurred when the temperature had a decreasing trend.

When temperature and precipitation change simultaneously, the response of runoff and sediment yield was more complex than that associated with a single change. This complexity is related to the interaction of various factors affecting runoff and sediment yield. Under the trend of increasing temperature, the LAI values in all precipitation combinations were larger than those in 2000; thus, all the differences caused by vegetation cover changes were negative. Therefore, when the changes in runoff and sediment yield are negative because of reduced precipitation, vegetation cover changes will enhance the effects of climate changes on runoff and sediment yield; when the changes in runoff and sediment yield are positive because of increased precipitation, vegetation cover changes will inhibit the effects of climate changes on runoff and sediment yield.

According to the recent climate predictions, precipitation reduction trends are expected to continue in most parts of southwestern China as a result of global warming (Zhen et al., 2013; Sun et al., 2019). The results of the current study show that the annual runoff and sediment yield in the Zhenjiangguan Watershed decreased significantly in the

Table 8
Annual runoff and sediment yield changes caused by vegetation changes and their percentages to total changes while temperature and precipitation change simultaneously.

	Precipitation	Temperature					
		T + 0.7		T + 1.4		T + 2.1	
		Difference	Percentage	Difference	Percentage	Difference	Percentage
Annual runoff ($\times 10^6$ m^3)	P × (1 − 20%)	−4	0.9	−12	2.7	−21	4.4
	P × (1 − 10%)	−7	3	−16	6.1	−24	8.2
	P × (1 + 10%)	−13	−7.6	−22	−16.1	−32	−31.7
	P × (1 + 20%)	−16	−4.2	−25	−7.2	−35	−11.4
Annual sediment yield (metric tons)	P × (1 − 20%)	−1310	0.7	−4055	2.1	−7460	3.7
	P × (1 − 10%)	−2621	2.5	−6176	5.3	−8760	6.8
	P × (1 + 10%)	−7281	−8.4	−10,285	−14.5	−12,513	−22.8
	P × (1 + 20%)	−7424	−3.6	−12,954	−7	−17,535	−10.6

scenarios of temperature increase and precipitation decrease, which is consistent with the findings of many previous studies (Yan et al., 2018; Hou et al., 2018; Cheng et al., 2013). In addition to the direct effect of climate changes on hydrological processes within river basins, this paper also focuses on the climate-driven vegetation cover changes. In the case of temperature increase and precipitation decrease scenarios, when the synergistic changes of vegetation were introduced, the reduction of runoff and sediment yield in the watershed would increase slightly (the percentages of increase were within 10% of the total changes). The difference was caused by the increase of vegetation coverage under the trend of climate warming. Du and Shi (2013) revealed that runoff and sediment yield are positively correlated with the precipitation indices but negatively correlated with the vegetation indices. Their research showed that annual precipitation was the most important factor influencing the variation of runoff in Jinsha River Basin, followed by forest coverage, and their contributions to the variation of runoff were 69.8% and 17.3%, respectively. For sediment yield, rainfall erosivity was the most important factor, followed by forest coverage, and their contributions to the variation of sediment yield were 49.3% and 24.2%, respectively. The contributions of forest coverage to the variation of runoff and sediment yield shown by Du and Shi (2013) were greater than the contribution of vegetation coverage shown in the current study, which may be due to the difference of vegetation types between the two study areas.

4. Conclusions

In this paper, a regression model was established between climate change factors (temperature and precipitation) and vegetation change factors (NDVI), and a distributed hydrological model based on physical mechanisms was applied. The Zhenjiangguan Watershed was used to study runoff and erosion variations under the impact of synergetic changes in climate and vegetation, and the following conclusions were obtained:

(1) The analysis of the NDVI-climate regression model shows that the NDVI has a strong correlation with temperature and precipitation, where the multiple correlation coefficient was 0.75 and the adjusted coefficient of determination was 0.51. This regression model can be used for NDVI predictions for different climate change scenarios.
(2) Precipitation is the most sensitive factor affecting runoff and sediment yield in the watershed, and 10% annual precipitation change can cause 10%–14% change of annual runoff and 17%–24% change of annual sediment yield. Temperature is also an important factor affecting runoff and sediment yield in the watershed. Each 0.7 °C increase in temperature can result in decreases of 1.4%–2% in annual runoff and 2%–3.7% in annual sediment yield.
(3) The climate-driven changes in vegetation have an impact on runoff and sediment yield, and the magnitude and nature of this influence vary among different combinations of temperature and precipitation changes. When temperature was kept constant, the effect of vegetation cover change caused by precipitation change on runoff and sediment yield was relatively small (only 0.9%–1.5% of the total change), and vegetation cover change inhibited the effect of precipitation change on runoff and sediment yield. When precipitation was kept constant, the effect of vegetation cover change caused by temperature change on runoff and sediment yield was relatively large (20%–30% of the total change), and vegetation cover change enhanced the effects of temperature change on runoff and sediment yield. When temperature and precipitation changed simultaneously, under the trend of increasing temperature, vegetation change not only enhanced the impact of reduced precipitation on runoff and sediment yield, but also inhibited the impact of increased precipitation on runoff and sediment yield. This investigation considers the synergistic effects of climate and vegetation cover change, and thus further clarifies the extent to which climate change impacts water and ecological resources.

Acknowledgments

This study was supported by the 13th Five-Year National Key Research and Development Program of China (2016YFC0401407, 2016YFC0401401) and the National Natural Science Foundation of China (51722901). The authors thank the Computer Network Information Center, Chinese Academy of Sciences for providing the DEM data, the National Earth System Science Data Sharing Infrastructure for providing the land-use maps and the AVHRR NDVI data, the Environmental and Ecological Science Data Center for West China for providing the soil data, and the China Meteorological Data Sharing Service System for providing the meteorological data. The authors also express thanks to Liwen Bianji, Edanz Group China (www.liwenbianji.cn/ac), for editing the English text of a draft of this manuscript.

References

Abbaspour, K.C., Yang, J., Maximov, I., Siber, R., Bogner, K., Mieleitner, J., Srinivasan, R., 2007. Modelling hydrology and water quality in the pre-alpine/alpine Thur watershed using SWAT. J. Hydrol. 333, 413–430.
Andersen, H.E., Blicher-Mathiesen, G., Bechmann, M., Povilaitis, A., Iital, A., Lagzdins, A., 2014. Climate change and the potential effects on runoff and nitrogen losses in the Nordic–Baltic region. Agric. Ecosyst. Environ. 198, 114–126.
Arpe, K., Hagemann, S., Jacob, D., Roeckner, E., 2005. The realism of the ECHAM5 models to simulate the hydrological cycle in the Arctic and North European area. Hydrol. Res. 36, 349–367.
Beck, H.E., McVicar, T.R., van Dijk, A.I., Schellekens, J., Jeu, R.A., Bruijnzeel, L.A., 2011. Global evaluation of four AVHRR–NDVI data sets: Intercomparison and assessment against Landsat imagery. Remote Sens. Environ. 115, 2547–2563.
Chen, F., Dudhia, J., 2001. Coupling an advanced land surface–hydrology model with the Penn State–NCAR MM5 modeling system. Part I: model implementation and sensitivity. Mon. Weather Rev. 129, 569–585.
Cheng, L.I.U., Jueyi, S.U.I., Yun, H.E., Hirshfield, F., 2013. Changes in runoff and sediment load from major Chinese rivers to the Pacific Ocean over the period 1955–2010. Int. J. Sediment Res. 28, 486–495.
Cho, K.H., Pachepsky, Y.A., Kim, J.H., Kim, J.W., Park, M.H., 2012. The modified SWAT model for predicting fecal coliforms in the Wachusett Reservoir Watershed, USA. Water Res. 46, 4750–4760.
Dechmi, F., Burguete, J., Skhiri, A., 2012. SWAT application in intensive irrigation systems: model modification, calibration and validation. J. Hydrol. 470, 227–238.
Du, J., Shi, C.X., 2013. Modeling and analysis of effects of precipitation and vegetation coverage on runoff and sediment yield in Jinsha River Basin. Water Sci. Eng. 6, 44–58.
Flügel, W.A., 1995. Delineating hydrological response units by geographical information system analyses for regional hydrological modelling using PRMS/MMS in the drainage basin of the River Bröl, Germany. Hydrol. Process. 9, 423–436.
Fontana, F.M., Coops, N.C., Khlopenkov, K.V., Trishchenko, A.P., Riffler, M., Wulder, M.A., 2012. Generation of a novel 1 km NDVI data set over Canada, the northern United States, and Greenland based on historical AVHRR data. Remote Sens. Environ. 121, 171–185.
Fu, B., Burgher, I., 2015. Riparian vegetation NDVI dynamics and its relationship with climate, surface water and groundwater. J. Arid Environ. 113, 59–68.
Hou, J., Ye, A., You, J., Ma, F., Duan, Q., 2018. An estimate of human and natural contributions to changes in water resources in the upper reaches of the Minjiang River. Sci. Total Environ. 635, 901–912.
Hu, B.Y., Tang, J.P., Wang, S.Y., 2012. A numerical simulation for mid-21st century climate change over China under IPCC A1B scenario. J. Meteorol. Sci. 32, 127–136.
Jin, X., Hu, G., Li, W., 2008. Hysteresis effect of runoff of the Heihe River on vegetation cover in the Ejina Oasis in Northwestern China. Earth Sci. Front. 15, 198–203.
Kim, J.K., Onda, Y., Kim, M.S., Yang, D.Y., 2014. Plot-scale study of surface runoff on well-covered forest floors under different canopy species. Quat. Int. 344, 75–85.
LI, K.L., Jiang, J.J., Mao, R.Z., Ni, S.X., 2005. The modeling of vegetation through leaf area index by means of remote sensing. Acta Ecol. Sin. 6, 1491–1495.
Li, F., Zhang, Y., Xu, Z., Teng, J., Liu, C., Liu, W., Mpelasoka, F., 2013. The impact of climate change on runoff in the southeastern Tibetan Plateau. J. Hydrol. 505, 188–201.
Li, Z., Wu, W., Liu, X., Fath, B.D., Sun, H., Liu, X., Cao, J., 2017. Land use/cover change and regional climate change in an arid grassland ecosystem of Inner Mongolia, China. Ecol. Model. 353, 86–94.
Moriasi, D.N., Arnold, J.G., Van Liew, M.W., Bingner, R.L., Harmel, R.D., Veith, T.L., 2007. Model evaluation guidelines for systematic quantification of accuracy in watershed simulations. Trans. ASABE 50, 885–900.
Nash, J.E., Sutcliffe, J.V., 1970. River flow forecasting through conceptual models part I—A discussion of principles. J. Hydrol. 10, 282–290.
Neitsch, S.L., Arnold, J.G., Kiniry, J.R., Williams, J.R., 2011. Soil and Water Assessment

Tool Theoretical Documentation Version 2009. Texas Water Resources Institute.
Pang, G., Wang, X., Yang, M., 2017. Using the NDVI to identify variations in, and responses of, vegetation to climate change on the Tibetan Plateau from 1982 to 2012. Quat. Int. 444, 87–96.
Paus, A., 2013. Human impact, soil erosion, and vegetation response lags to climate change: challenges for the mid-Scandinavian pollen-based transfer-function temperature reconstructions. Veg. Hist. Archaeobotany 22, 269–284.
Pouchin, T., Debrie, J., Bourcier, A., 2002. Remote Sensing Images and the Normalized Difference Vegetation Index (NDVI) as a Means of Observing the Vegetation of West Africa. Sécheresse, France.
Pourmokhtarian, A., Driscoll, C.T., Campbell, J.L., Hayhoe, K., Stoner, A.M., Adams, M.B., Shanley, J.B., 2017. Modeled ecohydrological responses to climate change at seven small watersheds in the northeastern United States. Glob. Chang. Biol. 23, 840–856.
Routschek, A., Schmidt, J., Kreienkamp, F., 2014. Impact of climate change on soil erosion—a high-resolution projection on catchment scale until 2100 in Saxony/Germany. Catena 121, 99–109.
Senay, G.B., Elliott, R.L., 2000. Combining AVHRR-NDVI and landuse data to describe temporal and spatial dynamics of vegetation. For. Ecol. Manag. 128, 83–91.
Seneviratne, S.I., Corti, T., Davin, E.L., Hirschi, M., Jaeger, E.B., Lehner, I., Teuling, A.J., 2010. Investigating soil moisture–climate interactions in a changing climate: a review. Earth Sci. Rev. 99, 125–161.
Serpa, D., Nunes, J.P., Santos, J., Sampaio, E., Jacinto, R., Veiga, S., Abrantes, N., 2015. Impacts of climate and land use changes on the hydrological and erosion processes of two contrasting Mediterranean catchments. Sci. Total Environ. 538, 64–77.
Shrestha, N.K., Wang, J., 2018. Predicting sediment yield and transport dynamics of a cold climate region watershed in changing climate. Sci. Total Environ. 625, 1030–1045.
Simonneaux, V., Cheggour, A., Deschamps, C., Mouillot, F., Cerdan, O., Bissonnais, Y.L., 2015. Land use and climate change effects on soil erosion in a semi-arid mountainous watershed (high Atlas, Morocco). J. Arid Environ. 122, 64–75.
Sun, S., Li, Q., Li, J., Wang, G., Zhou, S., Chai, R., Lou, W., 2019. Revisiting the evolution of the 2009–2011 meteorological drought over Southwest China. J. Hydrol. 568, 385–402.
Tang, Z., Ma, J., Peng, H., Wang, S., Wei, J., 2017. Spatiotemporal changes of vegetation and their responses to temperature and precipitation in upper Shiyang River Basin. Adv. Space Res. 60 (5), 969–979.
Vicente-Serrano, S.M., Gouveia, C., Camarero, J.J., Beguería, S., Trigo, R., López-Moreno, J.I., Morán-Tejeda, E., 2013. Response of vegetation to drought time-scales across global land biomes. Proc. Natl. Acad. Sci. 110, 52–57.
Wen, X., Liu, Z., Lei, X., Lin, R., Fang, G., Tan, Q., Quan, J., 2018. Future changes in Yuan River ecohydrology: individual and cumulative impacts of climates change and cascade hydropower development on runoff and aquatic habitat quality. Sci. Total Environ. 633, 1403–1417.
Yan, D., Schneider, U.A., Schmid, E., Huang, H.Q., Pan, L., Dilly, O., 2013. Interactions between land use change, regional development, and climate change in the Poyang Lake district from 1985 to 2035. Agric. Syst. 119, 10–21.
Yan, X., Bao, Z., Zhang, J., Wang, G., He, R., Liu, C., 2018. Quantifying contributions of climate change and local human activities to runoff decline in the upper reaches of the Luanhe River basin. J. Hydro Environ. Res. https://doi.org/10.1016/j.jher.2018.11.002.
Yao, J., Wang, Y., Su, W., Luo, P.N., 2006. Fuzzy assessment of ecological vulnerability along upper reaches of Mingjiang River. Sci. Technol. Manag. Land and Resour. 2, 020.
Yesuf, H.M., Assen, M., Alamirew, T., Melesse, A.M., 2015. Modeling of sediment yield in Maybar gauged watershed using SWAT, northeast Ethiopia. Catena 127, 191–205.
Yu, X., Zhang, X., Li, J., Zhang, M., Xie, Y., 2006. Effects of vegetation cover and precipitation on the process of sediment produced by erosion in a small watershed of Loess Region. Acta Ecol. Sin. 26, 1–8.
Yu, W., Zang, S., Wu, C., Liu, W., Na, X., 2011. Analyzing and modeling land use land cover change (LUCC) in the Daqing City, China. Appl. Geogr. 31, 600–608.
Zhang, X.C., Nearing, M.A., 2005. Impact of climate change on soil erosion, runoff, and wheat productivity in central Oklahoma. Catena 61, 185–195.
Zhang, Y., Gao, J., Liu, L., Wang, Z., Ding, M., Yang, X., 2013a. NDVI-based vegetation changes and their responses to climate change from 1982 to 2011: a case study in the Koshi River Basin in the middle Himalayas. Glob. Planet. Chang. 108, 139–148.
Zhang, H., Li, D., Jiang, X., Wang, X., 2013b. Multiple-scale analysis of runoff-sediment tendency in Zhenjiangguan watershed based on stage characteristics. J. Hydroelectr. Eng. 3, 023.
Zhen, F.M., Jia, L., Shun, Q.Z., Wen, X.C., Shu, Q.Y., 2013. Observed climate changes in southwest China during 1961–2010. Adv. Clim. Chang. Res. 4, 30–40.
Zhou, G., Wei, X., Wu, Y., Liu, S., Huang, Y., Yan, J., Wang, C., 2011. Quantifying the hydrological responses to climate change in an intact forested small watershed in southern China. Glob. Chang. Biol. 17, 3736–3746.
Zhou, Y., Zhang, Y., Vaze, J., Lane, P., Xu, S., 2013. Improving runoff estimates using remote sensing vegetation data for bushfire impacted catchments. Agric. For. Meteorol. 182, 332–341.
Zoungrana, B.J., Conrad, C., Thiel, M., Amekudzi, L.K., Da, E.D., 2018. MODIS NDVI trends and fractional land cover change for improved assessments of vegetation degradation in Burkina Faso, West Africa. J. Arid Environ. 153, 66–75.